Research Article ISSN 2832-9384

Journal of Materials and Polymer Science

Spatial Problem of Non-Stationary Interaction of Narrow Stamp Into Two-Layer Base in Elastic-Plastic Formulation

Vladislav Bogdanov

Progressive Research Solutions Pty. Ltd.

***Corresponding author**

Vladislav Bogdanov,
Progressive Research Solutions Pty. Ltd.
28/2 Buller Rd, Artarmon, Sydney,
Australia 2064

Submitted : 27 March 2024 ; Published : 20 Aug 2024

Citation: Bogdanov, V.,(2024). Spatial Problem of Non-Stationary Interaction of Narrow Stamp Into Two-Layer Base in Elastic-Plastic Formulation. J mate poly sci, 4(3) :1-9. DOI : https://doi.org/10.47485/2832-9384.1059

Abstract

A generalized approach was developed for solving plane and spatial contact problems in a dynamic elastic-plastic formulation. The spatial problem of a strain stress state of a beam made from the composite reinforced two-layer material is being solved. The reinforced or armed composite material consists of two materials: the main material of glass and the reinforcing thin steel layer. Glass is a non-crystalline, often transparent amorphous solid, that has widespread practical and technological use in the modern industry. Glass has high strength and is not affected by the processes of aging of the material, corrosion, and creep. In addition, this material is cheap and widely available. The reinforced composite beam is rigidly linked to an absolutely solid base and on which an absolutely solid impactor acts from above in the centre on a small size of the area of initial contact.

Keywords: Spatial, strain, stress, state, impact, composite, armed, reinforced, material, elastic-plastic, deformation.

Introduction

The use of a generalized approach to solve dynamic contact problems in an elastic-plastic formulation makes it possible to use it to solve contact problems for a body of arbitrary shape, which is subjected to an arbitrary distributed over the contact zone or shock loading. For the design of composite and reinforced materials, a technique for solving dynamic contact problems in more adequate an elastic-plastic mathematical formulation is used. To consider the physical nonlinearity of the deformation process, the method of successive approximations is used, which makes it possible to reduce the nonlinear problem to a solution of the sequences of linear problems. Linear problems are solving using method of finite differences. Due to the developed approach, it is possible to use method of finite elements, analytical methods when plastic deformations from previous iterations consider in further steps. It is possible to use different criterions of plastic fluidity. For describing dynamic motion of solid environment, it is possible to use equations of the theory of dynamic of nano materials. In this case we would be able to simulate nano-effects and solve problems of nanotechnology. Using this approach, it is possible to solve impact problems, for that it is necessary to add Cauchy problem of moving impactor as solid body. All that is matter of further research.

Since glass is a cheap, ubiquitous material that is not susceptible to corrosion and aging and creep processes, like metals and alloys, the study of composite materials containing glass is relevant and actual.

In (Bogdanov, 2023; Bogdanov, 2022; Bogdanov, 2022; Bogdanov, 2023; Bogdanov, 2023), a new approach to solving the problems of impact and nonstationary interaction in the elastoplastic mathematical formulation was developed. In these papers like in non-stationary problems (Bogdanov, 2023; Bogdanov, 2022; Bogdanov, 2022; Bogdanov, 2023; Bogdanov, 2023), the action of the striker is replaced by a distributed load in the contact area, which changes according to a linear law. The contact area remains constant.

In (Bogdanov, 2022; Bogdanov, 2022; Bogdanov, 2023; Bogdanov, 2023) dynamic interaction process of plane hard body and two layers reinforced composite material was investigated and the fields of summary plastic deformations and normal stresses arising in the base are calculated using plane strain (Bogdanov, 2022; Bogdanov, 2022; Bogdanov, 2023; Bogdanov, 2023) and plane stress (Bogdanov, 2022; Bogdanov, 2023) states models. In (Bogdanov, 2022) results depend on the size of the area of an initial contact between the impactor and the upper surface of the base and depend on the thickness of the top metal layer of the composite base. In (Bogdanov, 2022) results were calculated depending on the material of top layer of the composite base. Composite bases reinforced by steel, titanium and aluminium top layers were investigated. In (Bogdanov, 2023) the problem of plane strain state of four-layer composite reinforced base was solved.

In contrast from the work (Bogdanov, 2022; Bogdanov, 2022; Bogdanov, 2023; Bogdanov, 2023; Bogdanov, 2018), in these papers, we investigate the impact process of hard body with base using spatial model.

Problem Formulation

Deformations and their increments (Bogdanov, 2023), Odquist parameter $\kappa = \int d\varepsilon_i^p$ (ε_i^p is plastic deformations intensity), stresses are obtained from the numerical solution of the dynamic elastic-plastic interaction problem of composite beam $\{-L/2 \le x \le L/2; 0 \le y \le B; -H \le z \le H\}$, in the plane of its cross section in the form of rectangle. Due to symmetry of the deformation process relative to the planes $x = 0$ and $z = 0$, below we will consider a parallelepiped $\Sigma = L \times B \times H$ (Fig.1) with two materials: main material is quarts glass $\{0 \le x \le L/2; 0 \le y \le B-h; 0 \le z \le H\}$ and steel $\{0 \le x \le L/2; B-h \le y \le B; 0 \le z \le H\}$ to solve the spatial problem. The contact between two layers is ideally rigid. The base contacts absolute hard half-space $\{y \le 0\}$. We assume that the contact between the lower surface of the base and the absolute hard half-space is ideally rigid.

From above on a body the rigid drummer contacting along a segment $\{0 \le x \le A; y = B; 0 \le z \le H\}$. Its action is replaced by an even distributed stress -P in the contact region, which changes over time as a linear function $P = p_{01} + p_{02}t$. The calculations use known methods for studying the quasi-static elastic-plastic (Bogdanov, 2023; Mahnenko, 1976; Mahnenko, 2003; Mahnenko et al., 2009) model, considering the non-stationarity of the load and using numerical integration implemented in the calculation of the dynamic elastic model (Bogdanov, 2023; Bogdanov, 2022; Bogdanov, 2022; Bogdanov, 2023; Bogdanov, 2023).

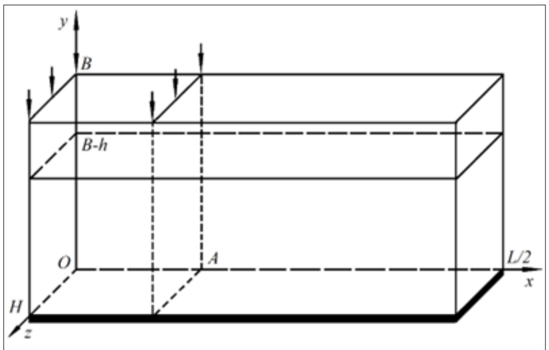

Figure 1: Geometric scheme of the problem

The equations of the spatial dynamic theory are considered, for which the components of the displacement vector $\mathbf{u} = (u_x, u_y, u_z)$ are related to the components of the strain tensor by Cauchy relations:

$$\varepsilon_{xx} = \frac{\partial u_x}{\partial x}, \quad \varepsilon_{xy} = \frac{1}{2}\left(\frac{\partial u_x}{\partial y} + \frac{\partial u_y}{\partial x}\right),$$
$$\varepsilon_{yy} = \frac{\partial u_y}{\partial y}, \quad \varepsilon_{xz} = \frac{1}{2}\left(\frac{\partial u_x}{\partial z} + \frac{\partial u_z}{\partial x}\right),$$
$$\varepsilon_{zz} = \frac{\partial u_z}{\partial z}, \quad \varepsilon_{yz} = \frac{1}{2}\left(\frac{\partial u_z}{\partial y} + \frac{\partial u_y}{\partial z}\right).$$

The equations of motion of the medium have the form:

$$\begin{aligned} &\frac{\partial \sigma_{xx}}{\partial x} + \frac{\partial \sigma_{xy}}{\partial y} + \frac{\partial \sigma_{xz}}{\partial z} = \rho \frac{\partial^2 u_x}{\partial t^2}, \\ &\frac{\partial \sigma_{xy}}{\partial x} + \frac{\partial \sigma_{yy}}{\partial y} + \frac{\partial \sigma_{yz}}{\partial z} = \rho \frac{\partial^2 u_y}{\partial t^2}, \\ &\frac{\partial \sigma_{xz}}{\partial x} + \frac{\partial \sigma_{yz}}{\partial y} + \frac{\partial \sigma_{zz}}{\partial z} = \rho \frac{\partial^2 u_z}{\partial t^2}. \end{aligned} \quad (1)$$

where p − material density.

The boundary and initial conditions of the problem have the form:

$$\begin{array}{llll} x=0, & 0<y<B, & 0<z<H: & u_x=0,\ \sigma_{xy}=0,\ \sigma_{xz}=0, \\ x=L/2, & 0<y<B, & 0<z<H: & \sigma_{xx}=0,\ \sigma_{xy}=0,\ \sigma_{xz}=0, \\ y=0, & 0<x<L/2, & 0<z<H: & \sigma_{yy}=0,\ \sigma_{xy}=0,\ \sigma_{yz}=0, \\ y=B, & 0<x<A, & 0<z<H: & \sigma_{yy}=-P,\ \sigma_{xy}=0,\ \sigma_{yz}=0, \\ y=B, & A<x<L/2, & 0<z<H: & \sigma_{yy}=0,\ \sigma_{xy}=0,\ \sigma_{yz}=0, \\ z=0, & 0<x<L/2, & 0<y<B: & \sigma_{zz}=0,\ \sigma_{xz}=0,\ \sigma_{yz}=0, \\ z=H, & 0<x<L/2, & 0<y<B: & \sigma_{zz}=0,\ \sigma_{xz}=0,\ \sigma_{yz}=0, \end{array} \quad (2)$$

$$\begin{aligned} &u_x\big|_{t=0} = 0,\ u_y\big|_{t=0} = 0,\ u_z\big|_{t=0} = 0, \\ &\dot{u}_x\big|_{t=0} = 0,\ \dot{u}_y\big|_{t=0} = 0,\ \dot{u}_z\big|_{t=0} = 0. \end{aligned} \quad (3)$$

The determinant relations of the mechanical model are based on the theory of non-isothermal plastic flow of the medium with hardening under the condition of Huber-Mises fluidity. The effects of creep and thermal expansion are neglected. Then, considering the components of the strain tensor by the sum of its elastic and plastic components (Bogdanov, 2023; Mahnenko, 1976), we obtain expression for them:

$$\begin{aligned} &\varepsilon_{ij} = \varepsilon_{ij}^e + \varepsilon_{ij}^p,\ d\varepsilon_{ij}^p = s_{ij} d\lambda, \\ &\varepsilon_{ij}^e = \frac{1}{2G} s_{ij} + K\sigma + \varphi. \end{aligned} \quad (4)$$

here $s_{ij} = \sigma_{ij} - \delta_{ij}\sigma$ – stress tensor deviator; δ_{ij} – Kronecker symbol; E – modulus of elasticity (Young's modulus); G – shear modulus; $K_1 = (1-2\nu)/(3E)$, $K = 3K_1$ – volumetric compression modulus, which binds in the ratio $\varepsilon = K\sigma + \phi$ volumetric expansion 3Ɛ (thermal expansion ϕ = 0); $\sigma = (\sigma_{xx} + \sigma_{yy} + \sigma_{zz})/3$ − mean stress; $d\lambda$ – some scalar function (Mahnenko, 1976), which is determined by the shape of the load surface and we assume that this scalar function is quadratic function of the stress deviator s_{ij} (Mahnenko, 1976; Mahnenko, 2003; Mahnenko et al., 2009).

$$d\lambda = \begin{cases} 0 \quad (f \equiv \sigma_i^2 - \sigma_S^2(T) < 0) \\ \dfrac{3d\varepsilon_i^p}{2\sigma_i} \quad (f = 0, df = 0) \\ (f > 0 - \text{inadmissible}) \end{cases}, \quad (5)$$

$$d\varepsilon_i^p = \frac{\sqrt{2}}{3}\left(\left(d\varepsilon_{xx}^p - d\varepsilon_{yy}^p\right)^2 + \left(d\varepsilon_{xx}^p - d\varepsilon_{zz}^p\right)^2 + \right.$$

$$\left. + \left(d\varepsilon_{yy}^p - d\varepsilon_{zz}^p\right)^2 + 6\left(\left(d\varepsilon_{xy}^p\right)^2 + \left(d\varepsilon_{xz}^p\right)^2 + \left(d\varepsilon_{yz}^p\right)^2\right)\right)^{1/2},$$

$$\sigma_i = \frac{1}{\sqrt{2}}\left(\left(\sigma_{xx} - \sigma_{yy}\right)^2 + \left(\sigma_{xx} - \sigma_{zz}\right)^2 + \right.$$

$$\left. + \left(\sigma_{yy} - \sigma_{zz}\right)^2 + 6\left(\sigma_{xy}^2 + \sigma_{xz}^2 + \sigma_{yz}^2\right)\right)^{1/2}. \qquad (6)$$

It should be noted that the developed algorithm makes it possible to use the function f in (5) not only in the form of a quadratic function (in this case, we obtain the plastic fluidity condition in the Huber-Mises form), however also in the form of a function containing terms of degree higher then second degree. This statement requires further research.

The material is strengthened with a hardening factor η^* ((Bogdanov, 2023; Bogdanov, 2022; Bogdanov, 2022; Bogdanov, 2023; Bogdanov, 2023; Mahnenko, 1976):

$$\sigma_S(T) = \sigma_{02}(T_0)\left(1 + \frac{\kappa(T)}{\varepsilon_0}\right)^{\eta^*}, \quad \varepsilon_0 = \frac{\sigma_{02}(T_0)}{E}, \qquad (7)$$

where T – temperature; κ – Odquist parameter, $T_0 = 20^{\circ}$C, η^*– hardening coefficient; $\sigma_S(T)$– yield strength after hardening of the material at temperature T.

Rewrite (4) in expanded form:

$$d\varepsilon_{xx} = d\left(\frac{\sigma_{xx} - \sigma}{2G} + K\sigma\right) + (\sigma_{xx} - \sigma)d\lambda,$$

$$d\varepsilon_{yy} = d\left(\frac{\sigma_{yy} - \sigma}{2G} + K\sigma\right) + (\sigma_{yy} - \sigma)d\lambda,$$

$$d\varepsilon_{zz} = d\left(\frac{\sigma_{zz} - \sigma}{2G} + K\sigma\right) + (\sigma_{zz} - \sigma)d\lambda,$$

$$d\varepsilon_{xy} = d\left(\frac{\sigma_{xy}}{2G}\right) + \sigma_{xy}d\lambda, \qquad (8)$$

$$d\varepsilon_{xz} = d\left(\frac{\sigma_{xz}}{2G}\right) + \sigma_{xz}d\lambda,$$

$$d\varepsilon_{yz} = d\left(\frac{\sigma_{yz}}{2G}\right) + \sigma_{yz}d\lambda.$$

Solution Algorithm

Let the nonstationary interaction (Bogdanov, 2023) occur in a time interval $t \in [0, t_*]$. Then for every moment of time t:

$$\varepsilon_{ii}^e = \frac{\sigma_{ii} - \sigma}{2G} + K\sigma, \quad \varepsilon_{ij}^e = \frac{\sigma_{ij}}{2G}, \quad \frac{d\varepsilon_{ii}^p}{dt} = \left(\sigma_{ii} - \sigma\right)\frac{d\lambda}{dt}, \quad \frac{d\varepsilon_{ij}^p}{dt} = \sigma_{ij}\frac{d\lambda}{dt} \quad (\not\Sigma_i; i, j = x, y, z) \qquad (9)$$

For numerical integration over time, Gregory's quadrature formula [1, 11] of order $m_1 = 3$ with coefficients D_n was used. For more precise calculations it is necessary to use formulas of higher order. After discretisation in time with nodes $t_k = k\Delta t \in [0, t_*]$ $(k = 0, K)$ for each value k we write down the corresponding node values of deformation increments:

$$\Delta\varepsilon_{xx,k} = B_1\sigma_{xx,k} + B_2(\sigma_{yy,k} + \sigma_{zz,k}) - b_{xx}, \quad \Delta\varepsilon_{xy,k} = B_3\sigma_{xy,k} - b_{xy},$$

$$\Delta\varepsilon_{yy,k} = B_1\sigma_{yy,k} + B_2(\sigma_{xx,k} + \sigma_{zz,k}) - b_{yy}, \quad \Delta\varepsilon_{xz,k} = B_3\sigma_{xz,k} - b_{xz},$$

$$\Delta\varepsilon_{zz,k} = B_1\sigma_{zz,k} + B_2(\sigma_{xx,k} + \sigma_{yy,k}) - b_{zz}, \quad \Delta\varepsilon_{yz,k} = B_3\sigma_{yz,k} - b_{yz},$$

$$B_1 = \frac{1}{3}\left(K + \frac{1}{G} + 2D_0\Delta\lambda_k\right), \quad B_2 = \frac{1}{3}\left(K - \frac{1}{2G} - D_0\Delta\lambda_k\right), \quad B_3 = \frac{1}{2G} + D_0\Delta\lambda_k,$$

$$b_{ij} = \frac{1}{2G}\sigma_{ij,k-1} + \delta_{ij}\left(K - \frac{1}{2G}\right)\sigma_{k-1} - \sum_{n=1}^{m_1} D_n\left(\sigma_{ij,k-n} - \delta_{ij}\sigma_{k-n}\right)\Delta\lambda_{k-n}. \qquad (10)$$

The solution of the system (10), gives expressions for the components of the stress tensor at each step [1]:

$$\sigma_{xx,k} = A_1\Delta\varepsilon_{xx,k} + A_2\Delta\varepsilon_{yy,k} + A_2\Delta\varepsilon_{zz,k} + Y_{xx},$$

$$\sigma_{yy,k} = A_2\Delta\varepsilon_{xx,k} + A_1\Delta\varepsilon_{yy,k} + A_2\Delta\varepsilon_{zz,k} + Y_{yy},$$

$$\sigma_{zz,k} = A_2\Delta\varepsilon_{xx,k} + A_2\Delta\varepsilon_{yy,k} + A_1\Delta\varepsilon_{zz,k} + Y_{zz},$$

$$\sigma_{xy,k} = A_3\Delta\varepsilon_{xy,k} + Y_{xy}, \quad Y_{xx} = A_1b_{xx} + A_2b_{yy} + A_2b_{zz},$$

$$\sigma_{xz,k} = A_3\Delta\varepsilon_{xz,k} + Y_{xz}, \quad Y_{yy} = A_2b_{xx} + A_1b_{yy} + A_2b_{zz},$$

$$\sigma_{yz,k} = A_3\Delta\varepsilon_{yz,k} + Y_{yz}, \quad Y_{zz} = A_2b_{xx} + A_2b_{yy} + A_1b_{zz},$$

$$Y_{xy} = A_3b_{xy}, \quad Y_{xz} = A_3b_{xz},$$

$$Y_{yz} = A_3b_{yz}, \quad A_1 = (B_1 + B_2)\big/((B_1 - B_2)(B_1 + 2B_2)),$$

$$A_2 = -B_2\big/((B_1 - B_2)(B_1 + 2B_2)), \quad A_3 = 1/B_3. \qquad (11)$$

Function $\psi = 1/(2G) + \Delta\lambda$, which is characterizing the yield condition, taking into account (8), (9) and (11) is:

$$\psi = \begin{cases} \dfrac{1}{2G} \quad (f < 0) \\ \dfrac{1}{2G} + \dfrac{3\Delta\varepsilon_i^p}{2\sigma_i} \quad (f = 0, df = 0), \\ (f > 0 - \text{inadmissible}) \end{cases} \qquad (12)$$

$$\Delta\varepsilon_i^p = \frac{\sqrt{2}}{3}\left[\left(\Delta\varepsilon_{xx}^p - \Delta\varepsilon_{yy}^p\right)^2 + \left(\Delta\varepsilon_{xx}^p - \Delta\varepsilon_{zz}^p\right)^2 + \left(\Delta\varepsilon_{yy}^p - \Delta\varepsilon_{zz}^p\right)^2 + \right.$$

$$\left. + 6\left(\left(\Delta\varepsilon_{xy}^p\right)^2 + \left(\Delta\varepsilon_{xz}^p\right)^2 + \left(\Delta\varepsilon_{yz}^p\right)^2\right)\right]^{1/2}, \quad \Delta\varepsilon_{ij}^p = \Delta\varepsilon_{ij} - \Delta\varepsilon_{ij}^e, \quad (i, j = x, y, z).$$

To take into account (Bogdanov, 2023) the physical nonlinearity contained in conditions (12), the method of successive approximations is used, which makes it possible to reduce a nonlinear problem to a sequence of linear problems (Bogdanov, 2023; Mahnenko, 1976; Mahnenko, 2003; Mahnenko et al., 2009):

$$\psi^{(n+1)} = \left\{\psi^{(n)}p + \frac{1 - p}{2G}, \text{ if } \sigma_{iS} < -Q; \ \psi^{(n)}, \text{ if } -Q < \sigma_{iS} < Q; \ \psi^{(n)}\frac{\sigma_i^{(n)}}{\sigma_S(T)}, \text{ if } \sigma_{iS} > Q\right\},$$

$$\sigma_{iS} = \sigma_i^{(n)} - \sigma_S(T),$$

where Q – the value of the largest deviation of the stress intensity $\sigma_i^{(n)}$ in step n from the strengthened yield strength; n – is the approximation number.

The stresses and strains used above were determined for each unit cell from the numerical solution at each point in time $t_k = k\Delta t$.

Numerical Solution

For problem the explicit scheme of the finite difference method was used with a variable partitioning step along the axes Ox (M elements), Oy (N elements) and Oz (N_1 elements). The step between the split points was the smallest in the area of the layers contact and at the boundaries of the computational domain. Since the interaction process is fleeting, this did not affect the accuracy in the first thin layer, areas near the boundaries, and the adequacy of the contact interaction modelling.

The use of finite differences (Zukina, 2004; Hemming, 1972) with variable partition step for wave equations is justified in (Zukina, 2004), and the accuracy of calculations with an error of no more than $O\left((\Delta x)^2+(\Delta y)^2+(\Delta z)^2+(\Delta t)^2\right)$ where Δx, Δy, Δz and Δt – increments of variables: spatial x, y and z and time t. A low rate of change in the size of the steps of the partition mesh was ensured. The time step was constant.

The resolving system of linear algebraic equations with a banded symmetric matrix was solved by the Gauss method according to the Cholesky scheme.

In (Weisbrod & Rittel, 2000), during experiments, compact samples were destroyed in 21 – 23 *ms*. The process of destruction of compact specimens from a material of size and with contact loading as in (Weisbrod & Rittel, 2000) was modelled in a dynamic elastoplastic formulation as plane strain state, considering the unloading of the material and the growth of a crack according to the local criterion of brittle fracture. The samples were destroyed in 23 *ms*. This confirms the correctness and adequacy of the developed formulation and model.

Figs. 2 – 25 show the results of calculations of two-layer specimens which have a paralellepiped shape with a hardening factor of the material $\eta^* = 0, 05$. The main layer has made from quartz glass. The material of the reinforcing top thin layer is steel. Contact between glass and steel is an ideal rigid. Calculations were made at the following parameter values: temperature $T = 50^oC$; $L = 60$ *mm*; $B = 10$ *mm* ; $H = 25$ *mm* ; $h = 0.5$ *mm* ; $\Delta t = 3.21\text{-}10^{-8}$ *s*; $p_{01} = 8$ *Mpa* ; $p_{02} = 10$ *Mpa* ; $M = 22$; $N = 23$; $N_1 = 11$. The smallest splitting step was 0,01 *mm*, and the largest 9 *mm* ($\Delta x_{\min} = 0{,}02$ *mm*; $\Delta y_{\min} = 0{,}02$ *mm* $\Delta z_{\min} = 0{,}01$ *mm* (only the first layer); $\Delta x_{\max} = 7{,}1$ *mm* ; $\Delta y_{\max} = 0{,}94$ *mm* ; $\Delta z_{\max} = 9$ *mm*); contact zone was equal $a = 2A = a_1 = 3$ *mm* .

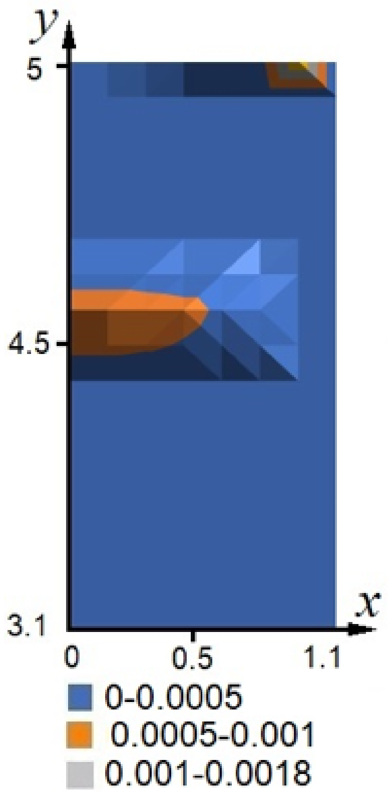

Figure 2: Odquist parameter κ when $x = x_1$ and $t = t_1$

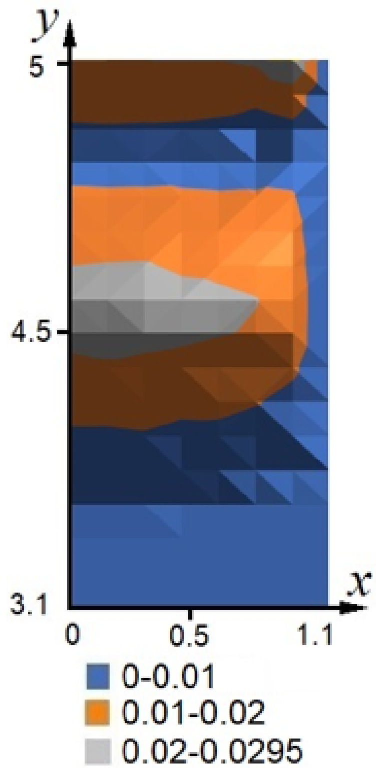

Figure 3: Odquist parameter κ when $x = x_1$ and $t = t_2$

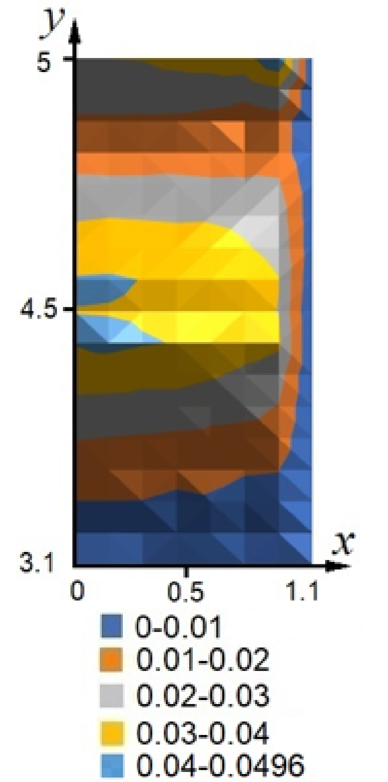

Figure 4: Odquist parameter κ when $x = x_1$ and $t = t_3$

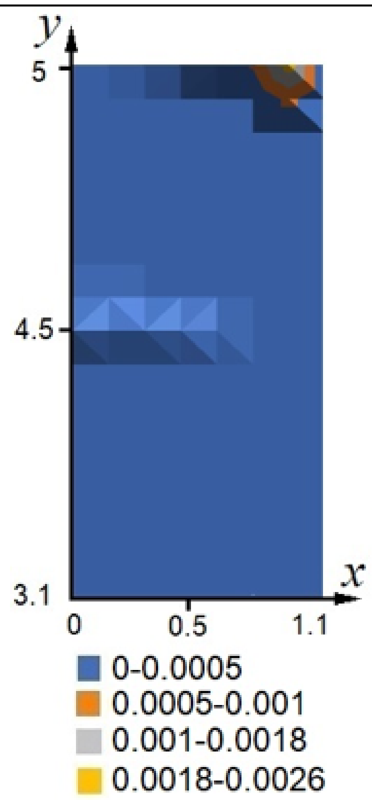

Figure 5: Odquist parameter κ when $x=x_2$ and $t=t_1$

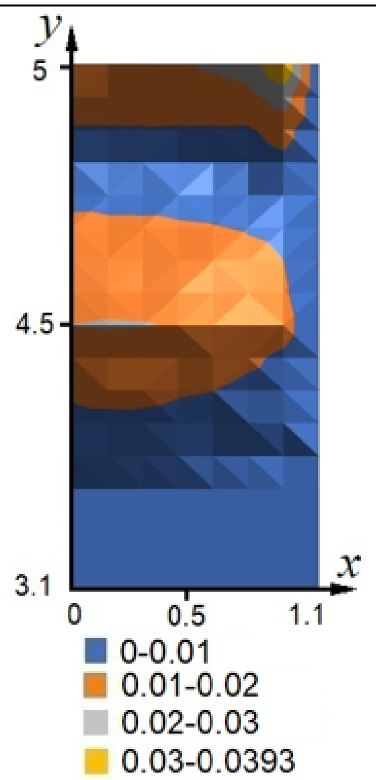

Figure 6: Odquist parameter κ when $x=x_2$ and $t=t_2$

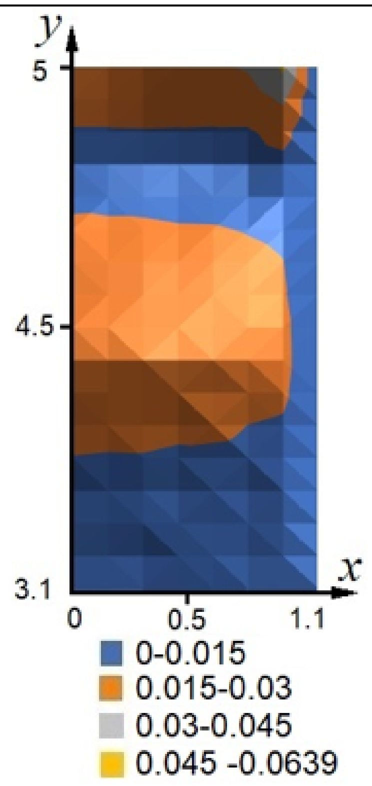

Figure 7: Odquist parameter κ when $x=x_2$ and $t=t_3$

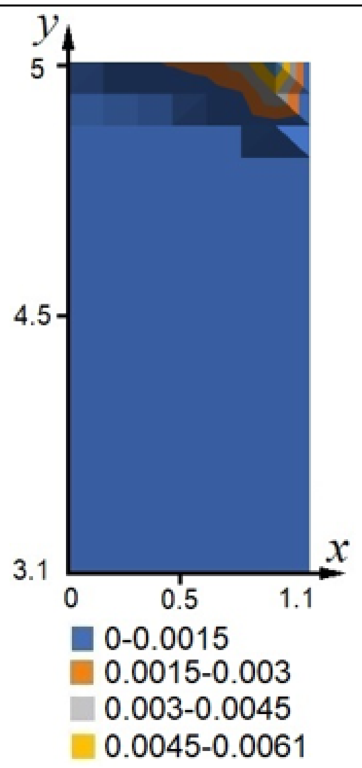

Figure 8: Odquist parameter κ when $x=x_3$ and $t=t_1$

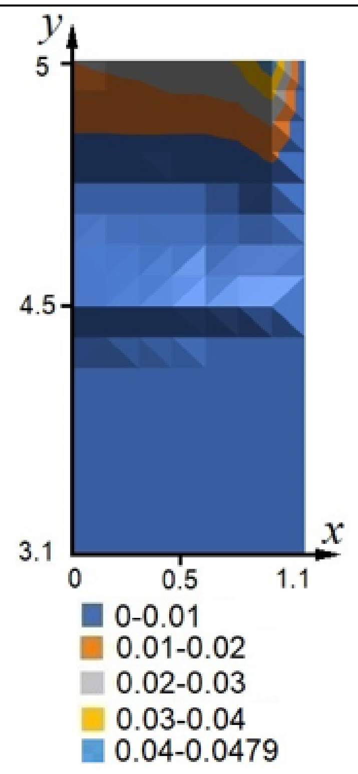

Figure 9: Odquist parameter κ when $x=x_3$ and $t=t_2$

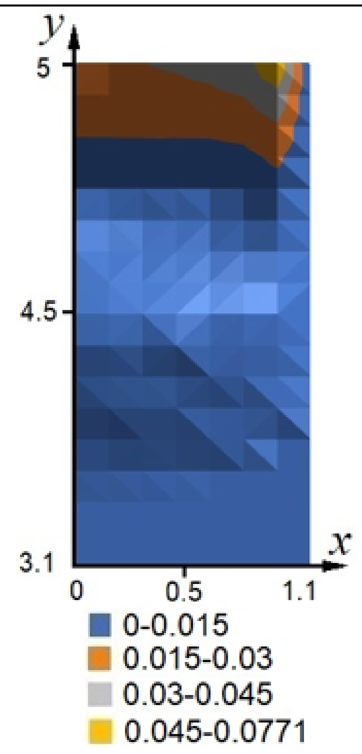

Figure 10: Odquist parameter κ when $x=x_3$ and $t=t_3$

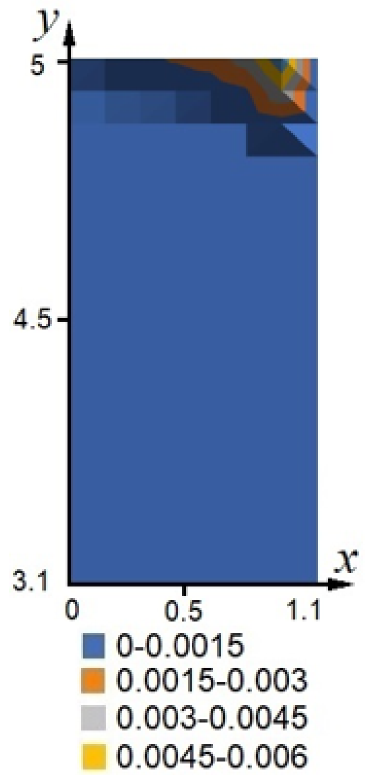

Figure 11: Odquist parameter κ when $x = x_4$ and $t = t_1$

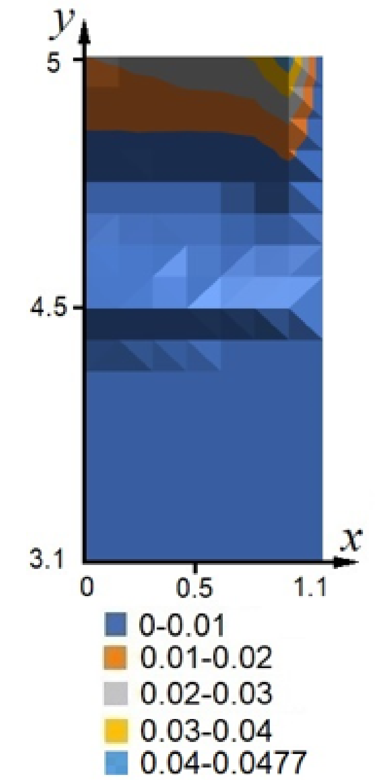

Figure 12: Odquist parameter κ when $x = x_4$ and $t = t_2$

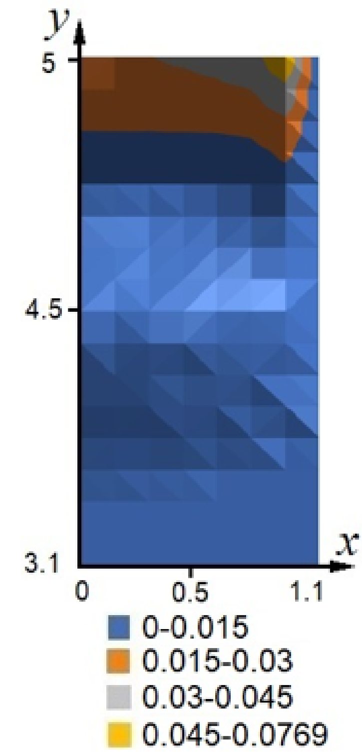

Figure 13: Odquist parameter κ when $x = x_4$ and $t = t_3$

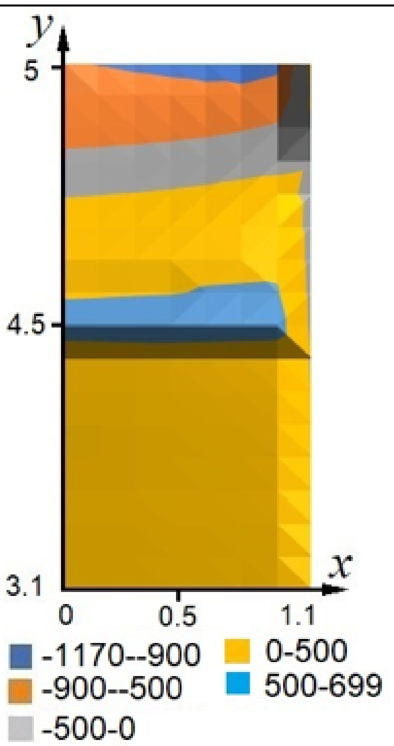

Figure 14: Stress σ_{xx} when $x = x_1$ and $t = t_1$

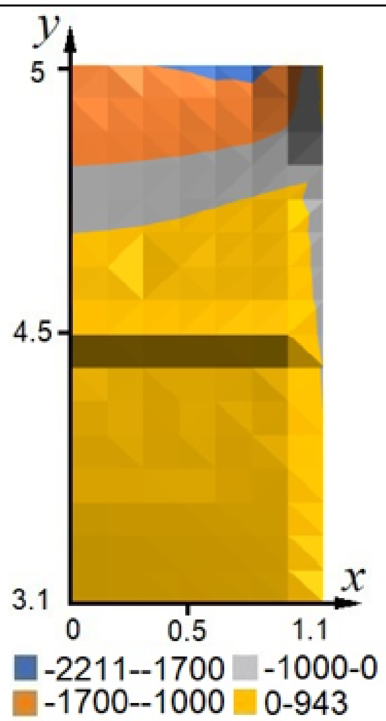

Figure 15: Stress σ_{xx} when $x = x_1$ and $t = t_2$

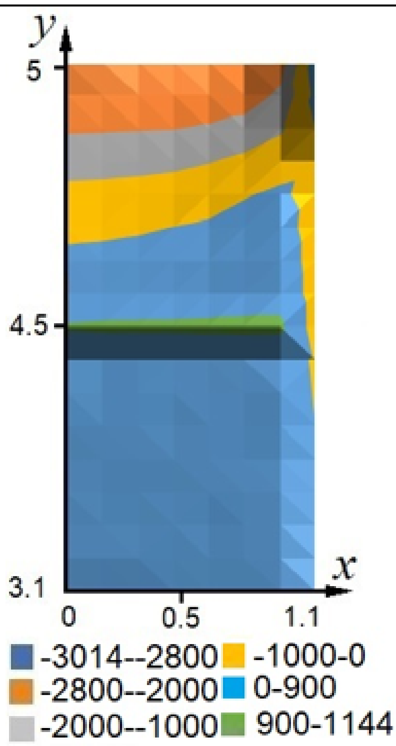

Figure 16: Stress σ_{xx} when $x = x_1$ and $t = t_3$

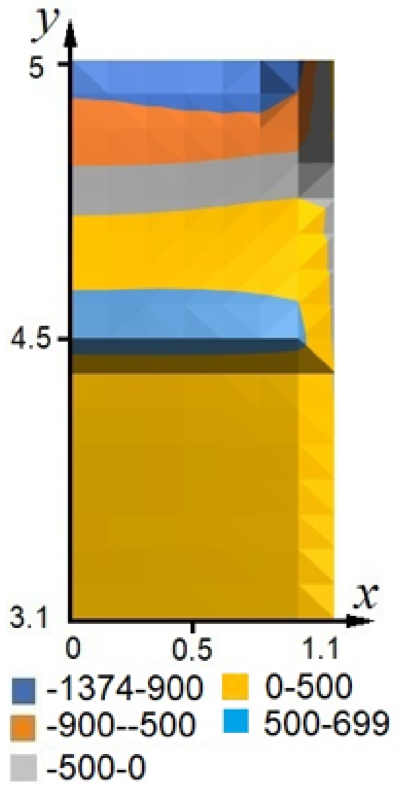

Figure 17: Stress σ_{xx} when $x = x_2$ and $t = t_1$

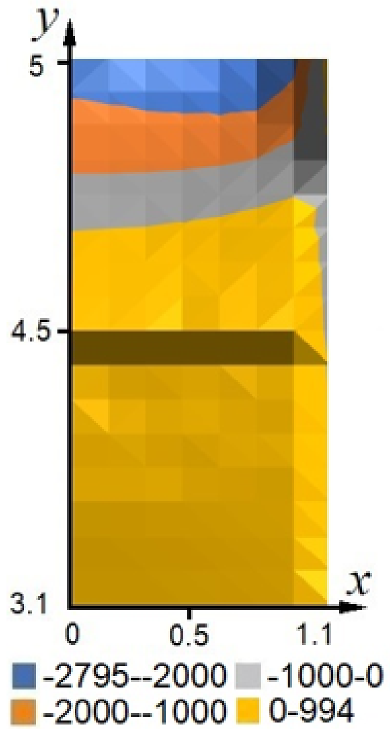

Figure 18: Stress σ_{xx} when $x = x_2$ and $t = t_2$

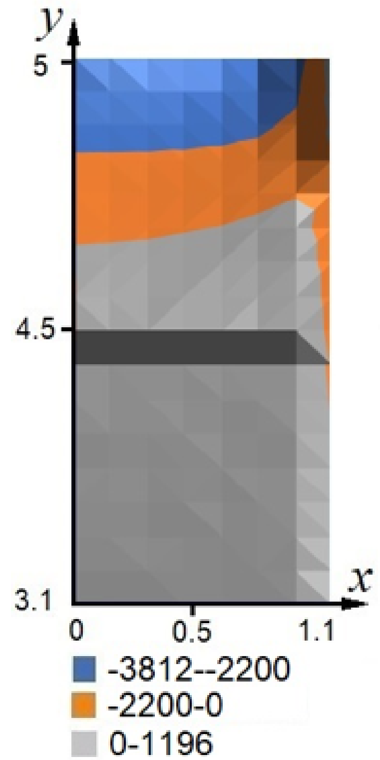

Figure 19: Stress σ_{xx} when $x = x_2$ and $t = t_3$

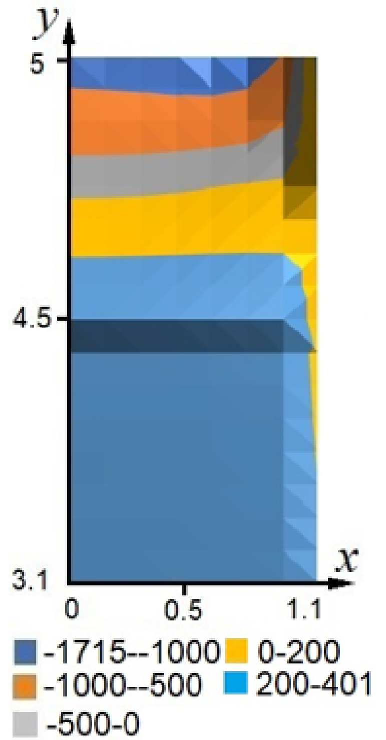

Figure 20: Stress σ_{xx} when $x = x_3$ and $t = t_1$

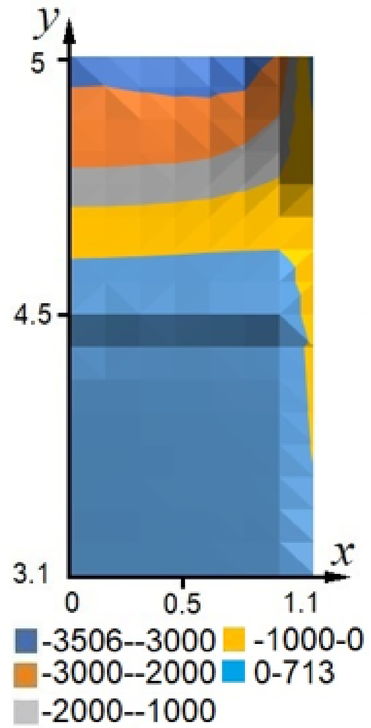

Figure 21: Stress σ_{xx} when $x = x_3$ and $t = t_2$

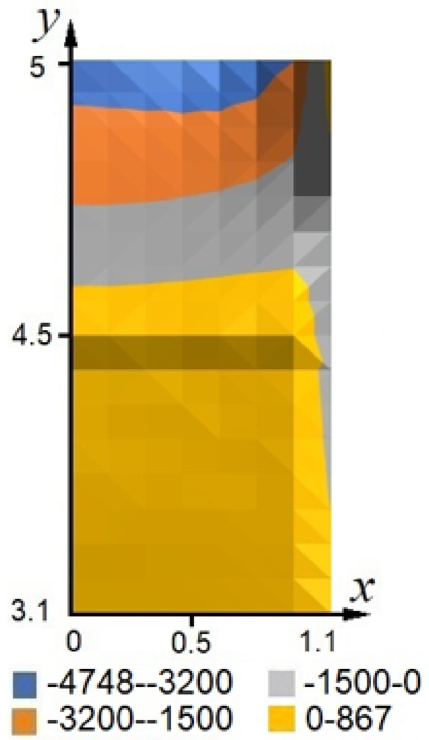

Figure 22: Stress σ_{xx} when $x = x_3$ and $t = t_3$

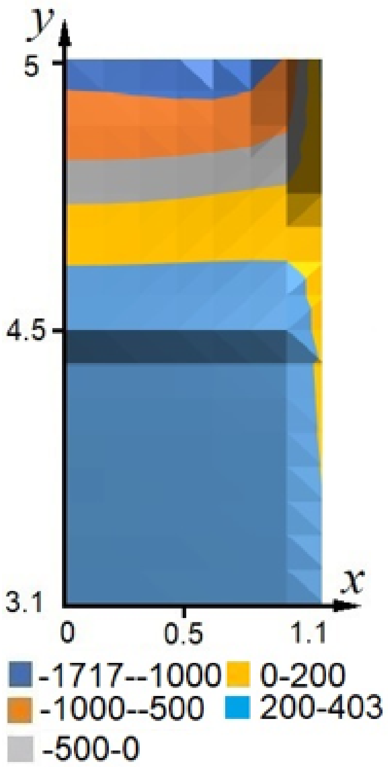

Figure 23: Stress σ_{xx} when $x = x_4$ and $t = t_1$

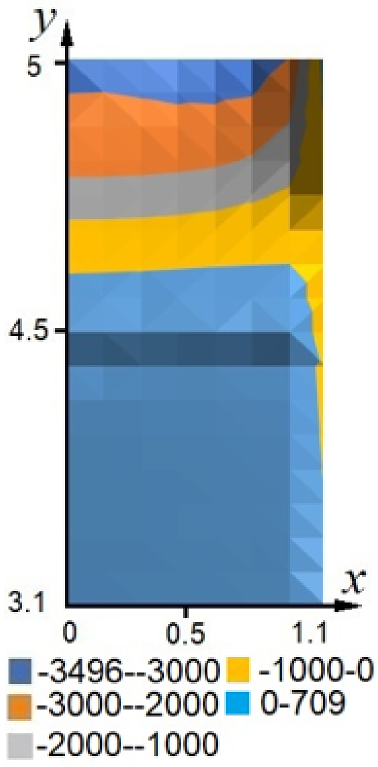

Figure 24: Stress σ_{xx} when $x = x_4$ and $t = t_2$

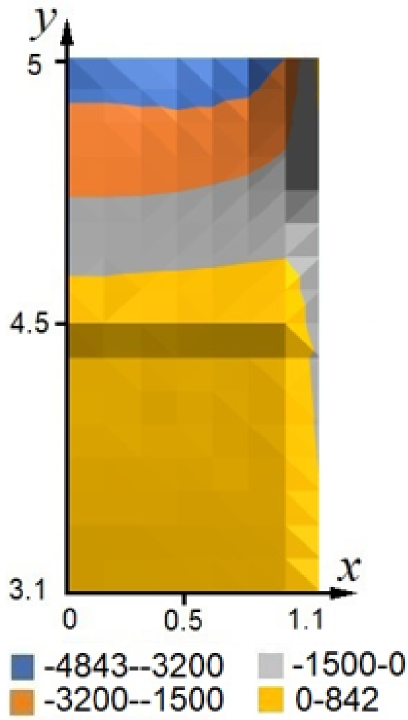

Figure 25: Stress σ_{xx} when $x = x_4$ and $t = t_3$

Figs. 2 – 13 and, 14 – 25 show the fields of the Odquist parameter κ and, normal stresses σ_{xx} at the times $t_1 = 0.64 \cdot 10^{-6}$ s, $t_2 = 1.92 \cdot 10^{-6}$ s and $t_3 = 2.89 \cdot 10^{-6}$ s in planes x_1= 49.98 *mm*, x_2= 49.88 *mm*, x_3= 43.3 *mm*, x_4= 27.3 *mm*, respectively.

As can be seen from Fig. 2–25, the greatest plastic deformations and stresses occur directly under the end of contact zone between the striker and base and in the area near the boundary of materials contact, which work as a concentrator of stresses and deformations. The largest values of the Odquist parameter and stresses occur in plane x_3= 43.3 *mm*. In the area of top steel layer which is under the stamp and above the boundary of contact two layer the large tensile stresses occur. This is due to the fact that the contacts between the layers and the lower boundary of the specimen with an absolutely rigid base are ideally rigid and process of stress propagation has a wave pattern. When a layer of glass is reinforced with a top layer of steel, stresses and deformations have a structure more similar to waves in the top layer.

Conclusions

The developed methodology of solving dynamic spatial contact problems in an elastic-plastic dynamic mathematical formulation makes it possible to model the processes of impact, shock and non-stationary contact interaction with the elastic composite base adequately. In this work, the process of impact on a two-layer base reinforced by thin top steel layer is adequately modelled and investigated relative to the small enough contact area size. The fields of parameter Odquist and normal stresses arising in the base are calculated. The numerical results confirm the need to strengthen the glass layer with a thin layer of steel/metal on the upper surface of the base (Bogdanov, 2022; Bogdanov, 2022; Bogdanov, 2023; Bogdanov, 2023). The boundary of contact between layers redistributes the stresses and plastic deformations that occur in such composite base. Normal stresses are concentrated in the area of top steel layer. The results obtained make it possible to design the narrow strips of new composite reinforced armed materials.

References

1. Bogdanov, V. (2023). Problems of impact and non-stationary interaction in elastic-plastic formulations. *Cambridge Scholars Publishing*. 282. https://www.cambridgescholars.com/product/978-1-5275-9339-8
2. Bogdanov, V. R. (2022). Problem of plane strain state of two-layer body in dynamic elastic-plastic formulation (Part I). *Underwater Technologies*, 12, 3-14. DOI: https://doi.org/10.32347/uwt.2022.12.1101
3. Bogdanov, V. R. (2022). Problem of plane strain state of two-layer body in dynamic elastic-plastic formulation (Part III). *International scientific journal "Transfer of Innovative Technologies", 5*(1), 62-70. DOI: https://doi.org/10.32347/tit.2022.51.0302
4. Bogdanov, V. (2023). Plane strain and stress states of two-layer composite reinforced body in dynamic elastic-plastic formulation. *Journal of Materials and Polymer Science, 3*(2), p. 1-7. DOI: doi.org/10.47485/2832-9384.1029

5. Bogdanov V. (2023). Plane strain state of four-layers composite reinforced body in dynamic elastic-plastic formulation. *Journal of Materials and Polymer Science, 3*(2), p. 1-7. DOI: doi.org/10.47485/2832-9384.1032
6. Bogdanov, V. R. (2018). Impact a circular cylinder with a flat on an elastic layer. *Transfer of In-novative Technologies, 1*(2), 68-74, DOI: 10.31493/tit1812.0302. Retrieved from http://tit.knuba.edu.ua/article/view/275917
7. Mahnenko, V. I. (1976). Computational methods for studying the kinetics of welding stresses and deformations. Naukova Dumka, Kiev, 320 (in Russian).
8. Mahnenko, V. I. (2003). Improving methods for estimating the residual life of welded joints in long-life structures. Automatic welding, Kiev, 10–11, 112–121 (in Russian).
9. Mahnenko, V. I., Pozniakov, V. D., Velikoivanenko, E. A., Rozynka, G. F. & Pivtorak, N. I. (2009). Risk of cold cracking when welding structural high-strength steels, Collection of scientific works "Processing of materials in mechanical engineering", National Shipbuilding University, 3, 5–12 (in Russian).
10. Zukina, E. L. (2004). Conservative difference schemes on non-uniform grids for a two-dimensional wave equation. Work of N.I. Lobachevski Math. Centre, Kazan, .26, 151–160 (in Russian).
11. Hemming, R. V. (1972). Numerical methods, Nauka, Moscow, 399 (in Russian).
12. Weisbrod, G. & Rittel, D. (2000). A method for dynamic fracture toughness determination using short beams. International Journal of Fracture, 104, 89–103.